Multiple controls regulate nucleostemin partitioning between nucleolus and nucleoplasm

Lingjun Meng[1], Hiroaki Yasumoto[1] and Robert Y. L. Tsai[1,*]

[1]Center for Cancer and Stem Cell Biology, Alkek Institute of Biosciences and Technology, Texas A&M Health Science Center, 2121 W Holcombe Blvd, Houston, TX 77030-3303, USA

*Author for correspondence (e-mail: rtsai@ibt.tamhsc.edu)

Accepted 6 October 2006
Journal of Cell Science 119, 5124-5136 Published by The Company of Biologists 2006
doi:10.1242/jcs.03292

Summary

Nucleostemin plays an essential role in maintaining the continuous proliferation of stem cells and cancer cells. The movement of nucleostemin between the nucleolus and the nucleoplasm provides a dynamic way to partition the nucleostemin protein between these two compartments. Here, we show that nucleostemin contains two nucleolus-targeting regions, the basic and the GTP-binding domains, that exhibit a short and a long nucleolar retention time, respectively. In a GTP-unbound state, the nucleolus-targeting activity of nucleostemin is blocked by a mechanism that traps its intermediate domain in the nucleoplasm. A nucleostemin-interacting protein, RSL1D1, was identified that contains a ribosomal L1-domain. RSL1D1 co-resides with nucleostemin in the same subnucleolar compartment, unlike the B23 and fibrillarin, and displays a longer nucleolar residence time than nucleostemin. It interacts with both the basic and the GTP-binding domains of nucleostemin through a non-nucleolus-targeting region. Overexpression of the nucleolus-targeting domain of RSL1D1 alone disperses nucleolar nucleostemin. Loss of RSL1D1 expression reduces the compartmental size and amount of nucleostemin in the nucleolus. Our work reveals that the partitioning of nucleostemin employs complex mechanisms involving both nucleolar and nucleoplasmic components, and provides insight into the post-translational regulation of its activity.

Supplementary material available online at
http://jcs.biologists.org/cgi/content/full/119/24/5124/DC1

Key words: Nucleolus, Nucleoplasmic, Nucleostemin, Retention, RSL1D1, Stem cell

Introduction

The nucleolus is a subnuclear compartment organized around the tandem repeats of ribosomal DNAs. It has become evident that the nucleolus is a very dynamic organelle. All nucleolar components are engaged in complex movements (Andersen et al., 2005; Olson and Dundr, 2005). Most, if not all, nucleolar proteins shuttle between the nucleolus and the nucleoplasm at a relatively fast pace (Andersen et al., 2005; Chen and Huang, 2001; Dundr et al., 2000; Phair and Misteli, 2000; Tsai and McKay, 2005). Several nucleoplasmic proteins, such as p53 (Rubbi and Milner, 2000), telomerase reverse transcriptase (TERT) (Wong et al., 2002), the murine double minute protein (MDM2) (Weber et al., 1999), and the von Hippel-Lindau tumor suppressor protein (Mekhail et al., 2004; Mekhail et al., 2005), have been shown to associate with the nucleolar structure under physiological or pathological conditions, suggesting that it serves as a form of subcellular machinery to activate or inactivate proteins that may not always reside in it. Compartmentalization provides a fast and energy-conserving mechanism to modulate protein activities without changing their expression levels. The movement of nuclear proteins in and out of the nucleolus allows cells to respond to a variety of environmental stimuli in a fast and dynamic fashion (Carmo-Fonseca et al., 2000; Tsai, 2004).

The complexity of the molecular devices controlling the protein flux through the nucleolus is manifested in many aspects. Unlike proteins that travel to membrane-bound organelles, most nucleolar proteins do not share a consensus targeting sequence, and their nucleolar localization signal (NoLS) often overlaps with their nuclear localization signals (NLS) (Martel et al., 2006; Reed et al., 2006; Sheng et al., 2004; You et al., 2005). Within the nucleolus, distinct subdomains can be identified by their electron-dense properties and by the distribution of proteins or ribosomal RNAs (Politz et al., 2002; Politz et al., 2005). In addition to their nucleolar-nucleoplasmic shuttling behavior, some nucleolar proteins might temporally associate with other subnuclear organelles, such as the Cajal body, paraspeckles, and the promyelocytic leukemia nuclear body (Bernardi et al., 2004; Fox et al., 2002; Sleeman et al., 2003). The dynamics of nucleolar proteins can be further modified by environmental signals, such as the pH (Mekhail et al., 2004) and the intracellular GTP level (Tsai and McKay, 2005). It remains unclear why and how these proteins move so rapidly between different nuclear compartments. Understanding the mechanisms underlying this process may provide insight into the regulation of nucleolar functions in protein synthesis, posttranscriptional modification of RNAs, cell-cycle progression, and stress response (Pederson, 1998; Rubbi and Milner, 2003).

The dynamic movement of the nucleolar protein nucleostemin is controlled by a GTP-driven cycle (Misteli, 2005; Tsai and McKay, 2005). Nucleostemin is highly enriched in the embryonic, mesenchymal, and neural stem cells, and several types of human cancers (Baddoo et al., 2003; Liu et al.,

2004; Tsai and McKay, 2002). It enters the nucleolus in a GTP-bound form, mediated in part by its basic (B) domain. When nucleostemin is in the GTP-unbound state, its nucleolar targeting ability is suppressed by the intermediate (I)-domain (Tsai and McKay, 2005). The GTP-binding capability of nucleostemin regulates its shuttling in and out of the nucleolus and, given its function in maintaining the proliferation of stem cells and cancer cells, may be used to transduce extracellular signals into the mitotic state of these cells in a fast and reversible manner. In this study, we attempted to dissect the protein(s) and structural components that regulate the compartmentalization of nucleostemin. We showed that the nucleolar localization of nucleostemin is mediated by its B-domain and GTP-binding (G)-domain, which interact with the gene ribosomal L1-domain-containing 1 (*RSL1D1*), belonging to the L1p/L10e family. RSL1D1 colocalizes with nucleostemin in the same subnucleolar domain and affects the nucleolar distribution of nucleostemin in the mutant-overexpression and small interference RNA (siRNA)-knockdown paradigms. By contrast, the movement of nucleostemin to the nucleolus is gated by a GTP-controlled mechanism that uses the I-domain as a nucleoplasmic anchor. Together, these mechanisms determine the partitioning of nucleostemin between the nucleolus and the nucleoplasm.

Results

Nucleostemin containes two nucleolar localization regions

Previously, we have shown that deletion of the B-domain in nucleostemin (NSdB) or the Gly256 to Val (G256V) point mutation reduces the nucleolar localization of nucleostemin, and that a combination of both [NSdB(G256V)] completely excludes it from the nucleolus (Tsai and McKay, 2005). To test whether the G-domain is sufficient to mediate nucleolar localization by itself, green fluorescent protein (GFP)-tagged nucleostemin mutants containing either the B-domain (B) or the G-domain, fused to an SV40 NLS (nlsG), or both (NSdA), were examined for their distribution in U2OS cells (Fig. 1A,B). Our results showed that the B- and the G-domain proteins were predominantly localized to the nucleolus (Fig. 1B, see B and nlsG). Nucleolar signal intensities relative to the nucleoplasmic intensities (N/P values) appeared stronger in the wild-type NS and the NSdA mutant that contain both the the B- and the G-domains than in the B and nlsG mutants that contain only one of the two domains (NS, 3.0; NSdA, 3.2; B, 2.0; nlsG, 1.9). To find out whether GTP-binding regulated the nucleolar localization of the nlsG mutant, we made a mutation on the conserved Gly256 residue in this mutant [nlsG(256)], and showed that this double mutant remained in the nucleolus. However, if the I-domain was included, the G256V mutation could disrupt the nucleolar distribution of the nlsGI mutant [nlsGI(256)]. In order to transport mutant proteins without NLS into the nucleus, a SV40 NLS (PKKKRKV) was engineered at the N-terminus of the G and GI mutants. This SV40 NLS did not display any nucleolar localization capability by itself when fused to a cytoplasmic hydrolase protein, yielding construct nlsHd3. These data demonstrate that both the B- and the G-domain possess nucleolus-targeting activities. The nucleolar localization of the G-domain alone does not require GTP-binding, but is gated by the I-domain in a GTP-dependent manner.

Long retention of nucleostemin in the nucleolus is mediated by its G-domain

Because the nucleolar residence time of the B-domain is much shorter than that of the full-length nucleostemin (Tsai and McKay, 2005), the G-domain might mediate the long retention of nucleostemin in the nucleolus. We confirmed this idea by the FRAP (fluorescence recovery after photobleaching) approach, which showed that the nucleolar retention time of the GI-domain was longer than that of the B-domain or the full-length nucleostemin (Fig. 1C1). The difference in FRAP between the GI-domain and the full-length nucleostemin could be attributed to the deletion of the acidic (A)-domain, because the GI-domain exhibited the same recovery kinetics as the NSdA mutant during the first 20 seconds after photobleaching (Fig. 1C2, 1C3). Thirty seconds after photobleaching, the GI-domain appeared to recover more fluorescence signals in the nucleolus than NSdA did. In these experiments, we included the I-domain because a deletion of this region prolonged the FRAP recovery time significantly and often caused cell death (Tsai and McKay, 2005). Because the I-domain has no nucleolar localization activity, we conclude that the G-domain is responsible for the long nucleolar retention of nucleostemin.

Nucleoplasmic retainment of nucleostemin is independent of the B- and G-domain

The I-domain might block the nucleolar localization of the GTP-unbound nucleostemin by masking its nucleolus-targeting regions or by a mechanism independent of the B- and G-domain, thereby retaining nucleostemin in the nucleoplasm. To determine which of the two mechanisms was used by nucleostemin, we first examined whether the I-domain can interact with the B- or G-domain. Using affinity binding assays, we showed that a fusion construct of glutathione S-transferase (GST) and the I-domain was unable to bind any of the B- or G-domain-containing mutants, regardless of their GTP-binding states (Fig. S1 in supplementary material). To determine whether the nucleoplasmic-retaining activity of the I-domain depended on the B- or G-domain, we tethered another nucleolar protein B23/nucleophosmin (B23) to an I-domain fragment at its N-terminus (myc-I-B23, Fig. 2A1) or C-terminus (B23-I-HA) (Fig. 2B1). Compared with the wild-type B23, the presence of the I-domain significantly increased the nucleoplasmic amount of B23 in the fusion mutant. This was not caused by the fusion per se, because Myc- or HA-tagged B23 proteins (Fig. 2A2 or 2B2, respectively) and B23 fused N- or C-terminally to GFP (239 residues versus 176 residues in the I-domain) showed wild-type B23 distribution (Fig. 2A3 versus 2B3, respectively). To further support these findings, we created I-domain fusion proteins of three ribosomal proteins, L5, L11 and L23, and showed that the I-domain can shift these proteins from a predominant nucleolar distribution to a nucleoplasmic distribution (Fig. 2C,D,E). These results demonstrate that the I-domain possesses the activity to retain nucleostemin in the nucleoplasm that is independent of the B- and G-domain.

Identification of a nucleostemin-interacting protein RSL1D1

To identify proteins involved in the nucleolar or nucleoplasmic retention of nucleostemin, a yeast two-hybrid screen was set up where a GAL4–DNA-binding-domain fusion of the GI-

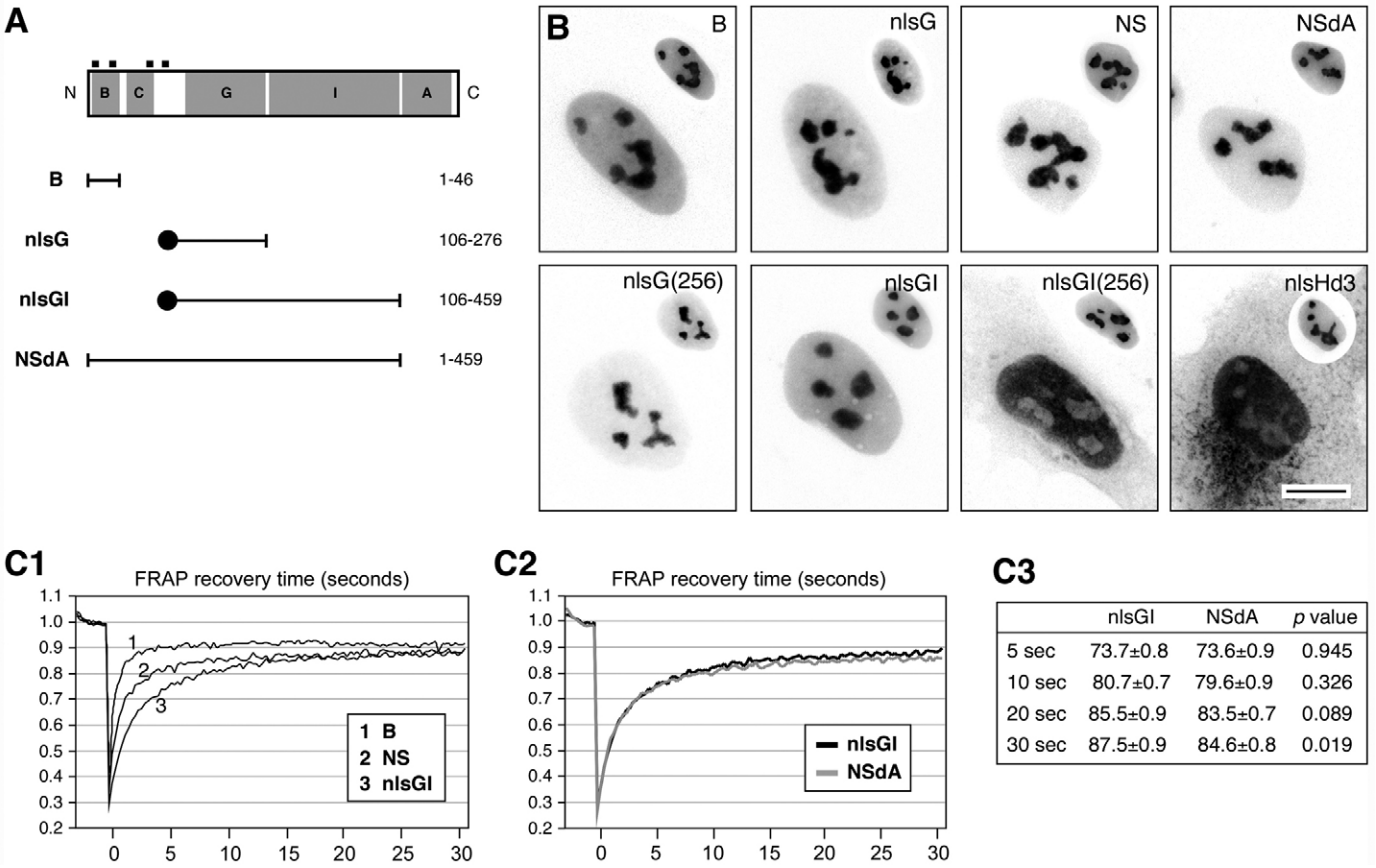

	nlsGI	NSdA	*p* value
5 sec	73.7±0.8	73.6±0.9	0.945
10 sec	80.7±0.7	79.6±0.9	0.326
20 sec	85.5±0.9	83.5±0.7	0.089
30 sec	87.5±0.9	84.6±0.8	0.019

Fig. 1. Nucleostemin containes two distinct nucleolus-targeting regions with different nucleolar retention time. (A) Diagram of nucleostemin (NS) protein structure and mutant constructs used to determine the nucleolus-targeting domains of nucleostemin. An SV40 nuclear localization signal (NLS, black circle) was introduced in mutants that lack an endogenous NLS (black boxes). Numbers indicate the aa positions. B, basic; C, coiled-coil; G, GTP-binding; I, intermediate; A, acidic. (B) Subcellular distributions of mutant proteins in U2OS cells were revealed by a C-terminal GFP-tag; counterstaining with anti-B23 antibody is shown in the right upper quadrants in all panels on a 50% scale. Both the B- and the G-domains (nlsG) displayed a nucleolar distribution pattern. Mutation of the conserved GTP-binding residue G256, yielding nlsG(256), did not affect the nucleolar localization of the G-domain alone. In the presence of the I-domain, such a mutation [nlsGI(256)] abolished its nucleolar localization. A cytoplasmic hydrolase protein (Hd3) was tagged with the SV40 NLS to demonstrate that this sequence was not sufficient to confer nucleolar localization. Bar, 10 μm. (C1) FRAP recovery times (*x*-axis, in seconds) of the B-domain (trace 1), the full-length nucleostemin (trace 2) and the GI-domain (trace 3) were determined in CHO cells transiently transfected with the GFP-fusion constructs. The *y*-axis represents the percentage of fluorescence intensity in the bleached area relative to the prebleached intensity. (C2) The FRAP recovery time of the GI-domain (nlsGI) and the A-domain deletion mutant (NSdA) was measured as described in the Materials and Methods. (C3) Statistical analyses at 5, 10, 20 and 30 seconds (mean ± standard error of mean (s.e.m.), n=20).

domain was used to screen a mouse embryonic day 7 (E7) cDNA library for potential binding proteins. From a total of 5.6 million clones screened, two positive ones were isolated. They encoded an in-frame full-length cDNA of the *RSL1D1* (GenBank accession number NM_025546.1) (Fig. 3A). The biochemical interaction between nucleostemin and RSL1D1 was shown by affinity binding assays in which the HA-tagged nucleostemin or RSL1D1 could be specifically retained by agarose-bound GST fusions of RSL1D1 (Fig. 3B1) or nucleostemin (Fig. 3B2), but not by the GST backbone protein. To confirm the interaction between nucleostemin and RSL1D1 in vivo, HEK293 cells were transfected with both HA-tagged nucleostemin and Myc-tagged RSL1D1 expression plasmids for coimmunoprecipitation. Our results showed that nucleostemin can be co-purified with RSL1D1 by anti-Myc antibody but not by mouse IgG (Fig. 3C, first row). Similarly, RSL1D1 was detected in the nucleostemin protein complex precipitated by anti-HA antibody (third row). Finally, we demonstrated that endogenous nucleostemin in HEK293 cells and Myc-tagged RSL1D1 can be co-purified in the same protein complexes precipitated by nucleostemin antiserum (Fig. 3D, left panel) or by anti-Myc antibody (right panel), but not by the control preimmune serum or mouse IgG. These results show that nucleostemin and RSL1D1 can form a protein complex both in vitro and in vivo.

RSL1D1 colocalizes with nucleostemin in the same subnucleolar compartments, unlike the distribution of B23 and fibrillarin

To address whether the interaction between nucleostemin and RSL1D1 is physiologically relevant, we first characterized *RSL1D1* expression during embryogenesis and in the adult tissues. Developmental northern blots showed that the *RSL1D1* message is abundantly expressed in the E10.5 and E12.5

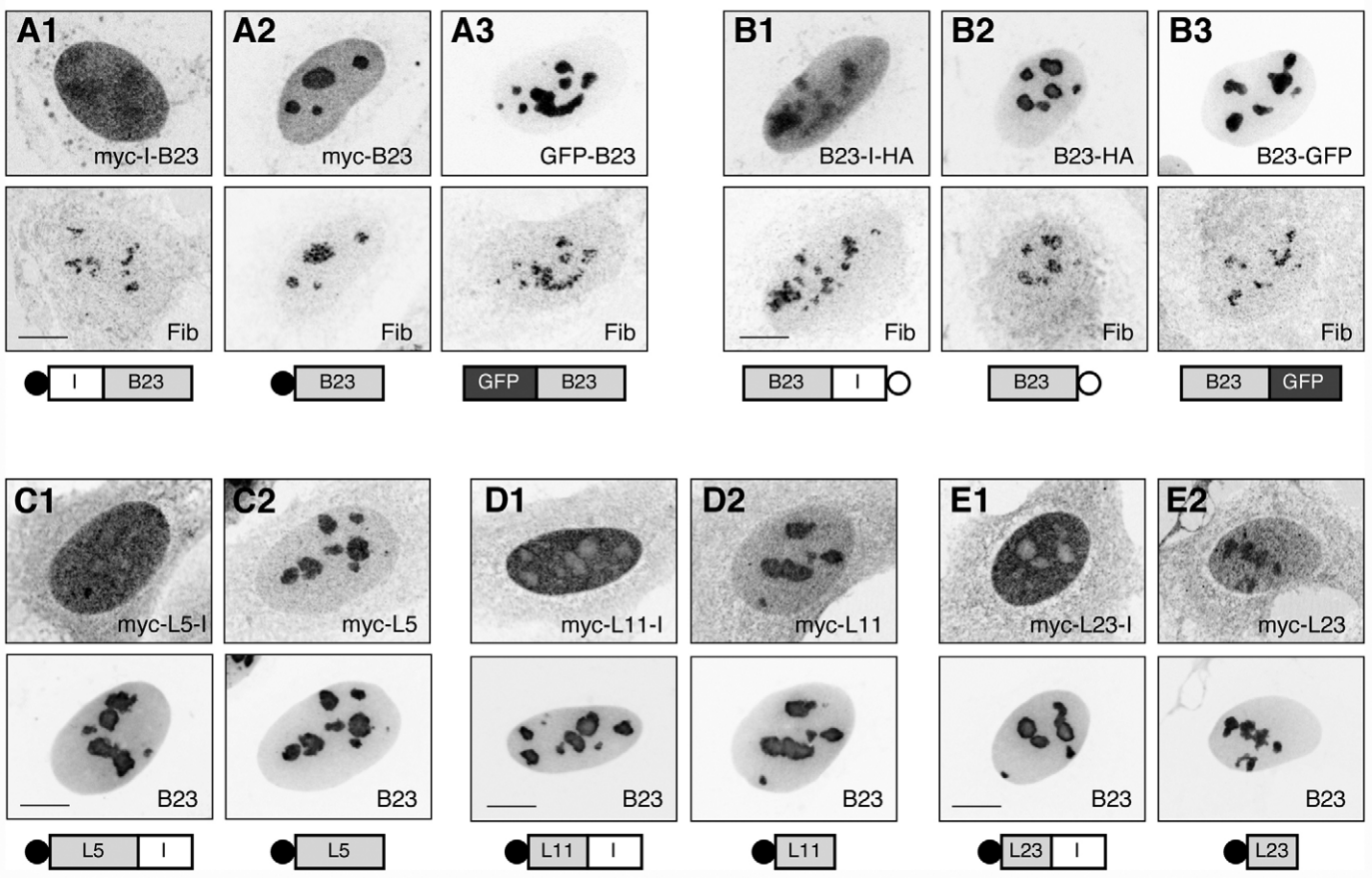

Fig. 2. The nucleolar localization of nucleostemin is gated by a nucleoplasmic-retaining mechanism independent of its nucleolus-targeting domains. (A1-E2) When fused to the N-terminus (A1) or the C-terminus (B1) of B23, the I-domain of nucleostemin significantly increased the amount of B23 in the nucleoplasm compared with the epitope-tagged (A2, B2) or the GFP-tagged proteins (A3, B3) at their respective ends. This nucleoplasmic-retaining activity of the I-domain could also be transferred to three ribosomal proteins, L5, L11 and L23. Unlike the nucleolar distributions of their original proteins (C2, D2, E2), the I-domain fusions of these proteins (C1, D1, E1) localized almost exclusively in the nucleoplasm. Anti-fibrillarin or anti-B23 immunostainings of the same cells are shown in the bottom panels. Fusion constructs are depicted at the bottom of each panel. Bars, 10 μm.

embryos and decreased after E12.5. This expression window overlapped with that of nucleostemin (Fig. 4A). In adult mice, *RSL1D1* was most expressed in the testis, followed by muscle and eye. Other tissues expressed *RSL1D1* at a low level (Fig. 4B). These results show that, the expression pattern of *RSL1D1* coincides with that of nucleostemin in the early embryos and in the adult testis (Tsai and McKay, 2002) and *RSL1D1* is more widely expressed than nucleostemin.

The subcellular distribution of RSL1D1 and nucleostemin was determined in U2OS cells by high-resolution confocal analyses. Our results showed that nucleostemin was non-uniformly distributed within the nucleolus (Fig. 4C1 and 4C2). To a great extent, the RSL1D1 signal, detected by a Myc epitope or GFP tag, co-localized with nucleostemin (Fig. 4C3 and supplementary material Fig. S2A). This distribution pattern was not identical to that of B23, which was less in the center and more in the periphery of the nucleolus (Fig. 4D and supplementary material Fig. S2B). Conversely, the subnucleolar domains where fibrillarin resided showed low nucleostemin and RSL1D1 signals (Fig. 4E and supplementary material Fig. S2C). These colocalization data provide a physiological basis for the nucleostemin-RSL1D1 interaction, and suggest a connection between the nucleolar localization of nucleostemin and RSL1D1.

RSL1D1 stays longer in the nucleolus than full-length nucleostemin

Next, we used FRAP experiments to determine how long RSL1D1 stayed in the nucleolus. A GFP-fusion of RSL1D1 was expressed in CHO cells. A FRAP paradigm was designed where a circle of 1 μm in diameter within the nucleolus was bleached (Fig. 5A, arrows), and the fluorescence recovery in the bleached area was recorded for 31.6 seconds (Fig. 5B). Our results showed that 5 seconds after photobleaching, the fluorescence recovery of RSL1D1 reached only 72.8% of the prebleached level, compared with the 80.9% recovery of nucleostemin (Fig. 5C). The FRAP recovery rate of RSL1D1 continued to lag behind that of nucleostemin throughout the 31.6-second recording period ($P<0.001$, $n=20$).

Nucleostemin-RSL1D1 interaction is mediated by the B- and G-domains of nucleostemin

To address whether the nucleostemin-RSL1D1 interaction is related to the nucleolus-targeting activity of nucleostemin, we

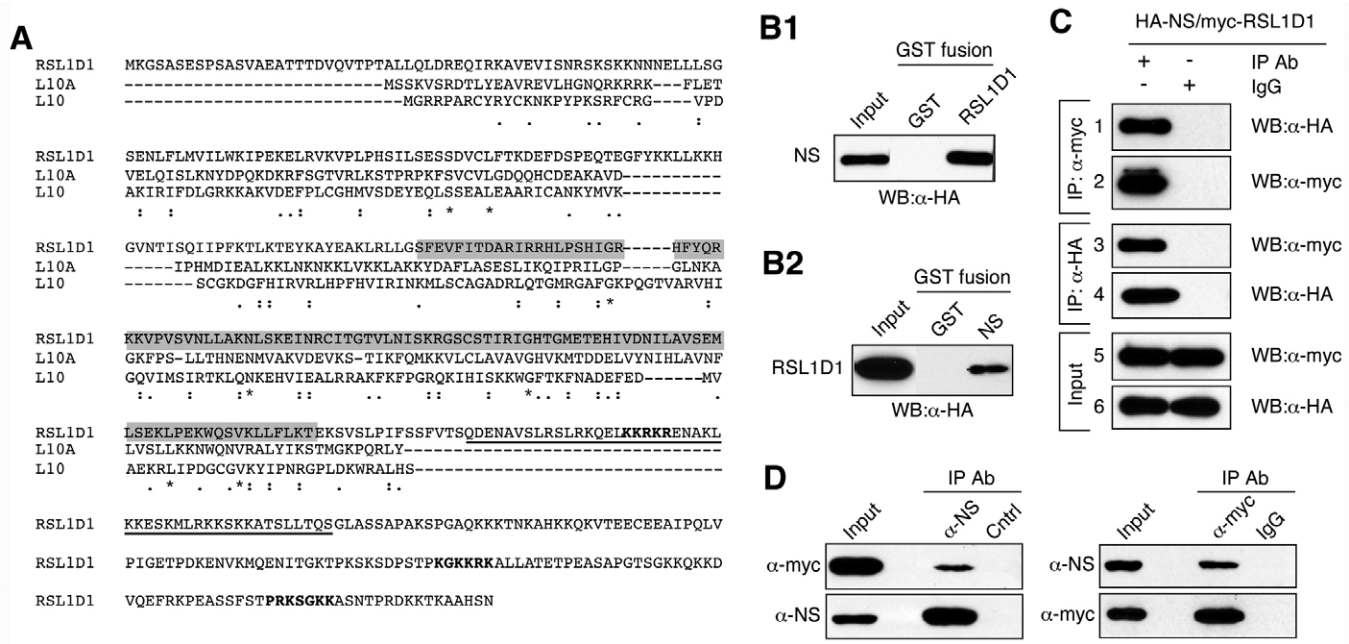

Fig. 3. Nucleostemin interacts with RSL1D1. (A) Protein sequences of mouse *RSL1D1* (GenBank accession no. NM_025546) and two closely related genes, *L10A* (GenBank accession no. NM_011287), and *L10* (GenBank accession no. XM_138143), were aligned by the Clustal W (1.81) program. Shaded and underlined areas represent the ribosomal L1 and the coiled-coil domain, respectively. Three putative NLS are marked in bold. *, fully conserved residues; **:**, conservation of strong groups; **.**, conservation of weak groups. Biochemical interaction between nucleostemin and RSL1D1 was shown by affinity binding assays using a GST-RSL1D1 fusion protein to pull down HA-tagged nucleostemin (B1) or a GST-nucleostemin fusion protein to pull down HA-tagged RSL1D1 (B2). (C) The nucleostemin-RSL1D1 interaction was confirmed by coimmunoprecipitation in both directions. HEK293 cells were co-transfected with HA-tagged nucleostemin and Myc-tagged RSL1D1 and immunoprecipitated with anti-Myc antibody (rows 1 and 2, left column, α-myc), anti-HA antibody (rows 3 and 4, rows, left column, α-HA), or mouse IgG (rows 1-4, right column). The co-purified proteins (rows 1 and 3) and the immunoprecipitates (rows 2 and 4) were detected by immunoblotting with the indicated polyclonal antibodies. (D) Left panel: Myc-tagged RSL1D1 was co-purified with endogenous nucleostemin in HEK293 cells by nucleostemin antiserum (α-NS), but not by preimmune serum (Cntrl). Right panel: endogenous nucleostemin was also be co-purified with Myc-tagged RSL1D1 by anti-Myc antibody (α-myc) but not by mouse IgG.

investigated which domains of nucleostemin are required for this interaction using a panel of truncated nucleostemin mutants (Fig. 6A). Affinity binding assays demonstrated that deletion of any single B-, C-, G-, I- or A-domain did not affect the binding of nucleostemin to RSL1D1, indicating that multiple regions are involved (Fig. 6B). Using complex deletion mutants, we showed that RSL1D1 interacts with both the BC- and the GI-domain individually, but very little or not at all with the G-, IA- or GI(256) mutants (Fig. 6C). The RSL1D1-binding domain of nucleostemin was further narrowed down to the B-domain of the BC mutant (Fig. 6D1) and to the GI1-domain of the GI mutant, consisting of the G-domain plus the N-terminal 73 residues of the I-domain (Fig. 6D2). Finally, we confirmed that the B- and G-domains are the major binding interfaces for RSL1D1. A double deletion of these two domains in nucleostemin (NSdBG) completely abolished the binding between nucleostemin and RSL1D1, whereas a double deletion of the C- and I-domains in nucleostemin (NSdCI) had no effect on the interaction between nucleostemin and RSL1D1 (Fig. 6D2). These results demonstrate that the RSL1D1-interacting and nucleolus-targeting domains of nucleostemin are the same.

Separate domains in RSL1D1 mediate its targeting to the nucleolus and its binding to nucleostemin

RSL1D1 contains an L1 domain (aa 150-254), a coiled-coil domain (aa 270-316) and three predicted NLS (Fig. 7A). To determine whether the nucleostemin-interacting domain of RSL1D1 overlaps with its nucleolar localization domain, we examined the nucleostemin-binding abilities and distribution patterns of the truncated RSL1D1 mutants (Fig. 7A). Affinity binding assays showed that GST fusions of the BC- and the GI-domain specifically retain the C-terminal half of RSL1D1 (aa 255-452), but not the N-terminal half mutant (aa 1-254) that includes the L1-domain (Fig. 7B). We further narrowed the nucleostemin-interacting domain of RSL1D1 down to its last 136 aa without the coiled-coil domain (aa 317-452). The distribution patterns of Myc-tagged truncated RSL1D1 mutants in relation to nucleostemin were determined by double-labeled immunofluorescence (Fig. 7C-L). The 150-316 aa region of RSL1D1, which contained the L1-domain, the coiled-coil domain and one NLS, was localized in the nucleolus (Fig. 7C). The 1-149 aa region by itself was distributed in the cytoplasm (Fig. 7D). When fused with an SV40 NLS, some of it entered the nucleolus (Fig. 7E). The nucleostemin-interacting 317-452 aa domain was diffusely localized in the nucleus (Fig. 7F) and, in some cells, displayed a slightly higher intensity in the nucleus than in the nucleoplasm (Fig. 7G). Further dissection of the nucleolus-targeting 150-316 aa region revealed that without an NLS, the L1 domain (aa 150-254) was trapped mostly in the cytoplasm. Only a small proportion of it was located around the nucleolus

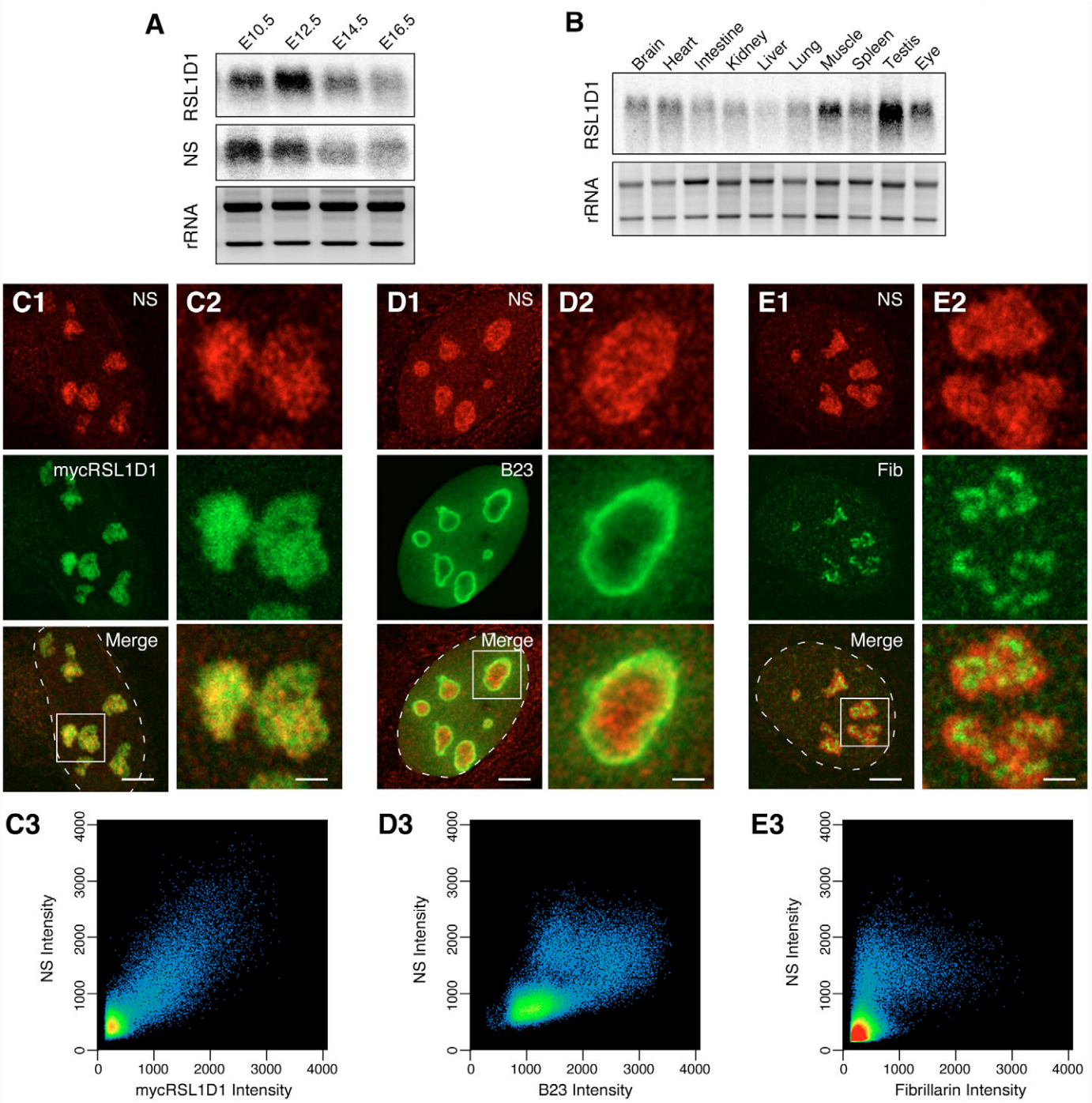

Fig. 4. Tissue and subcellular distributions of RSL1D1 overlap with those of nucleostemin. (A,B) Northern blot analyses of expression patterns of RSL1D1 and nucleostemin in the developing whole embryos from E10.5 to E16.5 (A) and in the adult mice (B). (C1-E3) Double-labeled immunofluorescence and confocal analyses showing colocalization of endogenous nucleostemin (NS, red) and Myc-tagged RSL1D1 (green) (C), NS (red) and B23 (green) (D), NS (red) and fibrillarin (Fib, green) (E). High magnifications of the indicated areas (squares) are shown in (C2, D2 and E2). Dashed lines delineate the nucleo-cytoplasmic boundaries. Bars, 5 μm for C1, D1, E1; 2 μm for C2, D2 and E2. Quantification of colocalization is shown in C3, D3 and E3. All pixels were plotted on the basis of their red (*y*-axis) and green (*x*-axis) fluorescence intensities, and pseudocolored on the basis of the event frequency, with red representing the highest and blue the lowest event frequency.

(Fig. 7H). When fused to an SV40 NLS, the nlsL1 mutant was able to enter the nucleolus (Fig. 7I). Notably, the nucleolar signal of nucleostemin was either diminished or absent in many cells expressing this nlsL1 mutant (Fig. 7J, bottom panel). The coiled-coil domain (aa 255-316) exhibited a diffuse nuclear distribution similar to that of the 317-452 aa region (Fig. 7K). Finally, except for the nlsL1 construct, neither the mutants nor the wild-type RSL1D1 (Fig. 7L) appeared to affect the

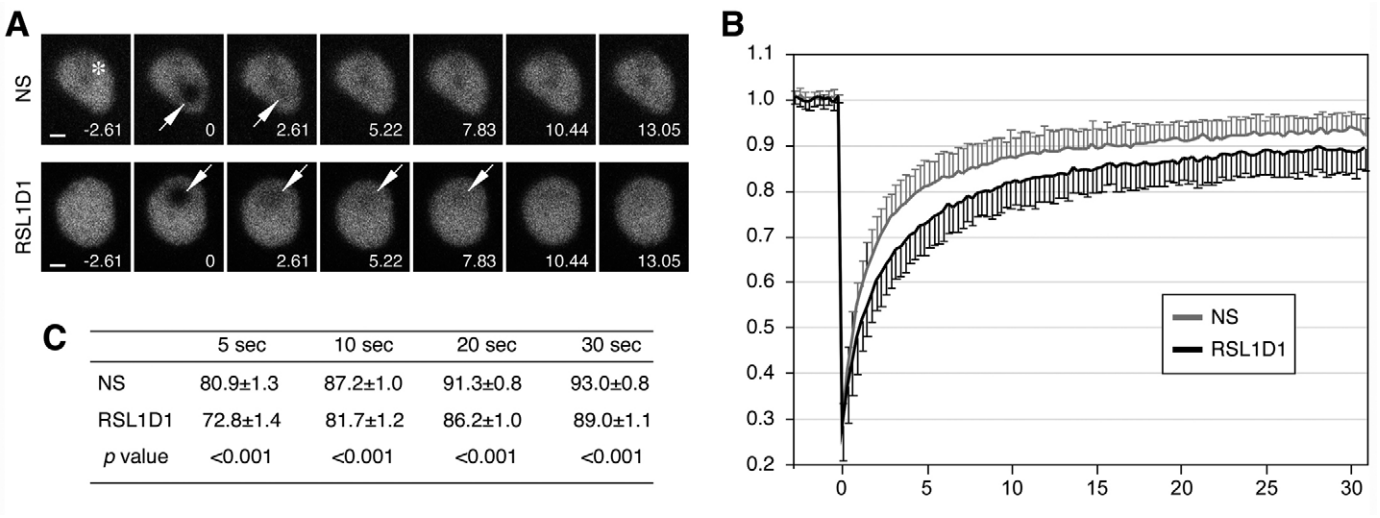

C

	5 sec	10 sec	20 sec	30 sec
NS	80.9±1.3	87.2±1.0	91.3±0.8	93.0±0.8
RSL1D1	72.8±1.4	81.7±1.2	86.2±1.0	89.0±1.1
p value	<0.001	<0.001	<0.001	<0.001

Fig. 5. RSL1D1 has a longer nucleolar retention time than nucleostemin. (A) Time-sequenced FRAP images of nucleostemin and RSL1D1 in the nucleolus. A circle of 1 μm in diameter within the nucleolus (arrows) was bleached. Of note, low intensity spots in the upper panels (*) existed before photobleaching. Numbers indicate the time in seconds after the bleaching event. Bars, 1 μm. (B) The FRAP recovery curves of RSL1D1 and nucleostemin depict the average of the fluorescence recovery level (*y*-axis; *n*=20) relative to the prebleached intensity (set as 1) over a 31.6-second period following photobleaching (*x*-axis) in seconds. Error bars represent ± standard deviations (±s.d.) and are omitted on the top and bottom side of the RSL1D1 and nucleostemin recovery curves for clarity. (C) *t*-test analyses of the FRAP results were conducted at 5, 10, 20 and 30 seconds after photobleaching (mean ± s.e.m.; *n*=20).

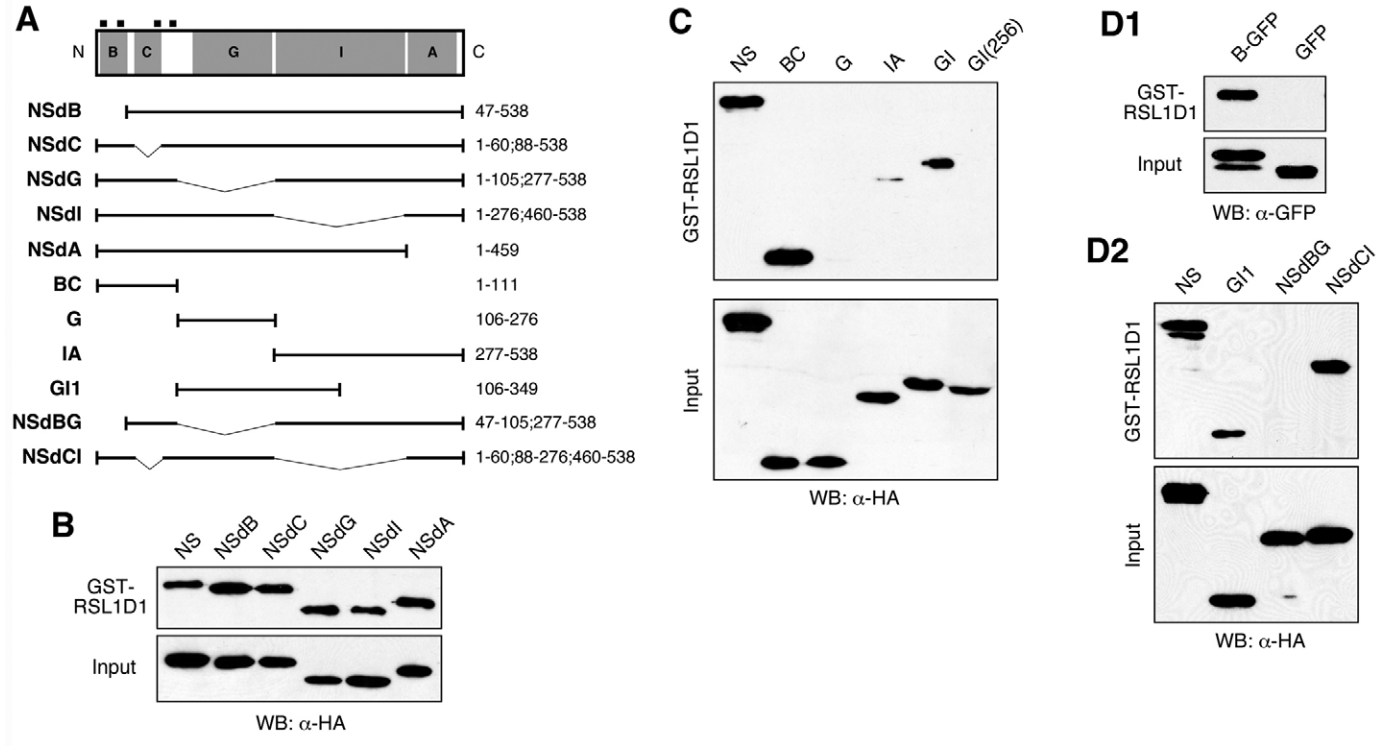

Fig. 6. RSL1D1 interacts with the B- and G-domains of nucleostemin. (A) Schematic diagrams of truncated nucleostemin mutants used to determine RSL1D1-interacting domain(s). (B) Affinity binding assays showing that GST fusions of RSL1D1 are able to pull down all single-domain deletion mutants of nucleostemin, suggesting involvement of multiple regions. (C) The use of truncation mutants showed that RSL1D1 binds both the BC- and the GI-domains, but not the G- and IA-domains or a GI-domain containing a G256V mutation (GI(256)). (D) Nucleostemin RSL1D1-binding domains were further narrowed down to the B-domain of the BC mutant (D1) and the GI1-domain of the GI mutant (D2). Double-deletion mutants (NSdBG and NSdCI) confirmed the importance of the B- and G-domains, but not of the C- and I-domains, in mediating the interaction of nucleostemin and RSL1D1 (D2).

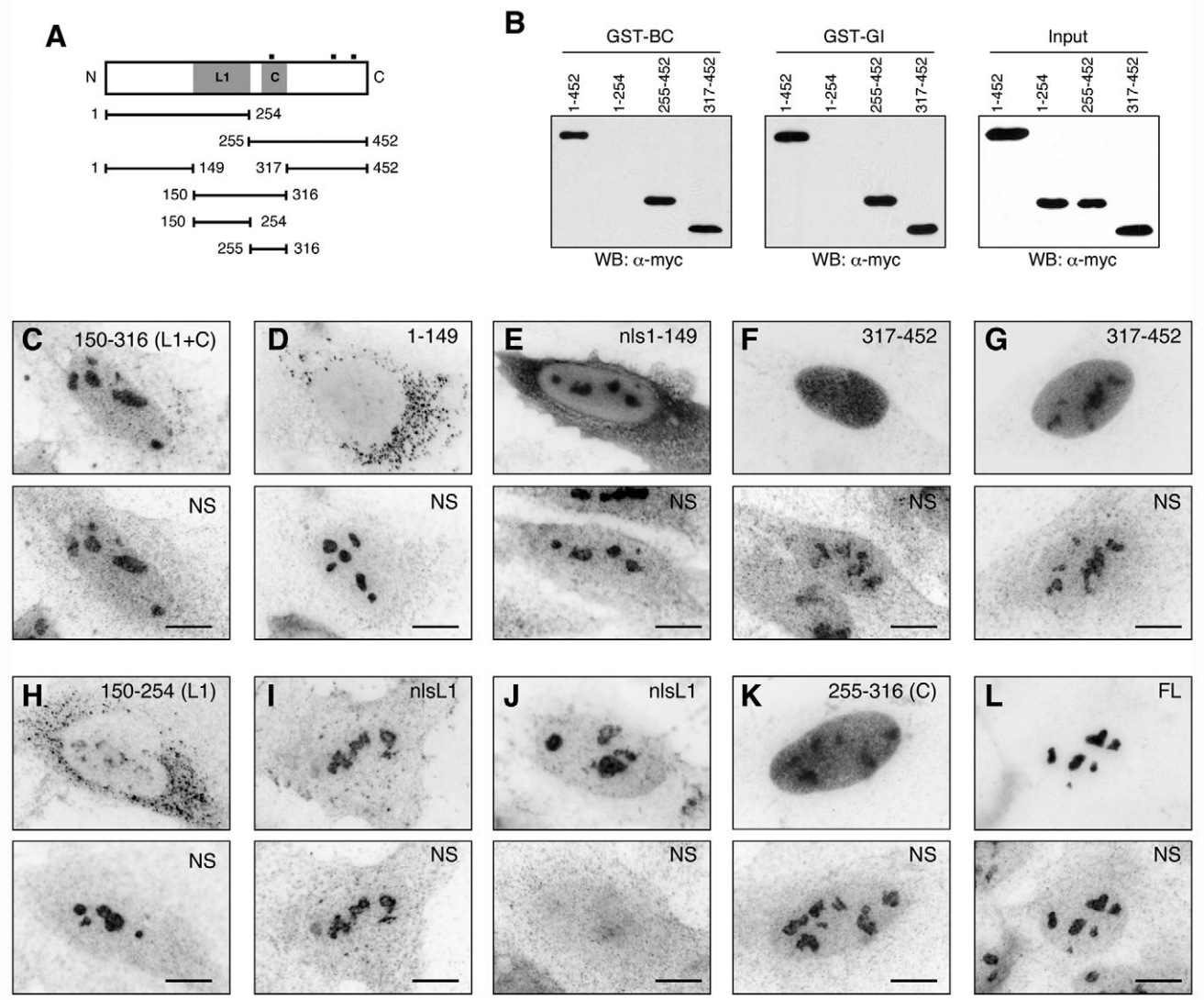

Fig. 7. Nucleolar distribution and the nucleostemin-interaction of RSL1D1 are controlled by separate domains. (A) RSL1D1 contains an L1 domain (aa 150-254), a coiled-coil domain (C) and three putative NLS (black boxes). Myc-tagged truncated RSL1D1 mutants were generated to map nucleostemin-interacting and nucleolus-targeting regions. (B) Affinity binding assays show that GST fusions of both the BC- and GI-domains bind the (aa 317-452) part of RSL1D1 that does not contain the L1- or C-domain. (C-L) Anti-Myc and anti-nucleostemin double-labeled immunofluorescence demonstrate that the 150-316 aa region of RSL1D1 is localized in the nucleolus (C). The N-terminal 1-149 aa region is cytoplasmic by itself (D), and becomes partially nucleolar when tagged with an SV40 NLS (E). Distribution of the C-terminal 317-452 aa region is diffuse in the nucleus (F), with some cells showing more signals in the nucleolus than in the nucleoplasm (G). Within the aa 150-316 segment, the L1 domain (150-254) by itself is primarily cytoplasmic (H), but becomes mostly nucleolar when fused to an SV40 NLS (I,J, nlsL1). The coiled-coil domain (255-316) is diffusely localized in the nucleus (K). The nucleostemin signal is diminished or absent from the nucleolus of many cells expressing nlsL1 (J). Bars, 10 μm.

distribution of endogenous nucleostemin (Fig. 7C-L, bottom panels). These data demonstrate that the nucleostemin-interacting domain of RSL1D1 contributes little to its nucleolar localization. Instead, the nucleolar distribution of RSL1D1 is mediated mostly by the L1-domain and partially by the 1-149 aa region, neither of which binds nucleostemin.

Overexpression of nlsL1 reduces the amount of nucleostemin in the nucleolus

The nlsL1 mutant was localized in the nucleolus, but lacked the ability to bind nucleostemin. Compared with non-transfected cells, overexpression of this mutant distinctively reduced the amount of nucleostemin in the nucleolus (Fig. 8A1). Despite its reduced intensity, the distribution pattern of the remaining nucleostemin signal in those cells resembled the nucleostemin distribution in non-transfected cells (Fig. 8A2). In some cells, the nucleostemin signals were scattered around the nlsL1 signals (Fig. 8B), indicating that overexpression of this mutant could lead to either a disruption of the nucleolar structure or a displacement of nucleostemin from its original compartment. To determine whether nlsL1 disrupts nucleolar organization, we examined its effect on the distributions of fibrillarin and B23, which are involved in pre-ribosomal RNA processing and ribosome maturation, respectively. Judging

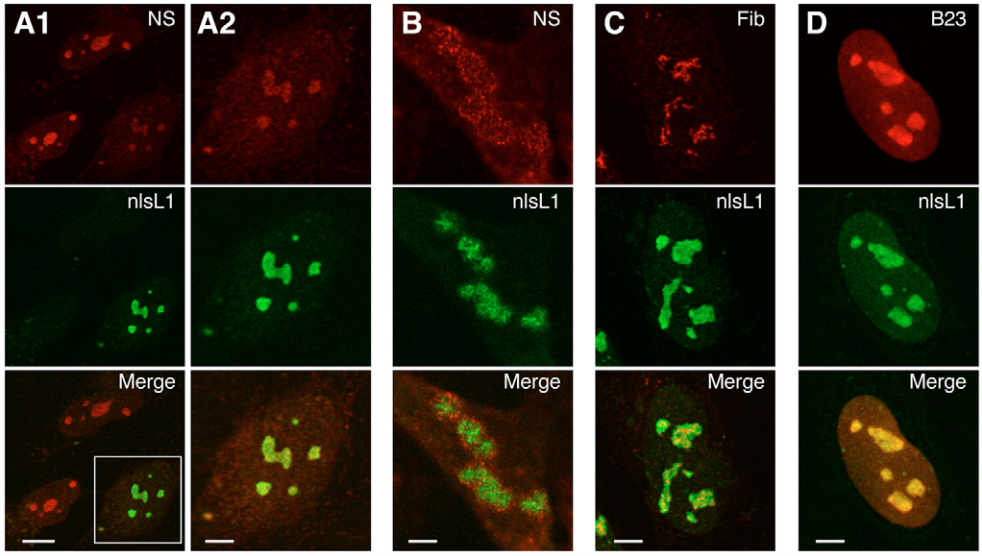

Fig. 8. Overexpression of a nucleolar form of the L1-domain (nlsL1) disperses nucleostemin from the nucleolus. (A1) The intensities of nucleostemin signals in the nucleolus are diminished or disappear in many cells that express the nlsL1 mutant. (A2) High magnification of the nlsL1-expressing cell show that its remaining nucleostemin signals display a reticular pattern of distribution, similar to the nucleostemin distribution in wild-type cells. (B) In some cells, nucleostemin is scattered around the nlsL1 signals. Overexpression of the nlsL1 mutant does not affect the signal intensities or the distribution patterns of fibrillarin (C) or B23 (D). Bars, 10 μm for A1; 5 μm for A2, B, C, D.

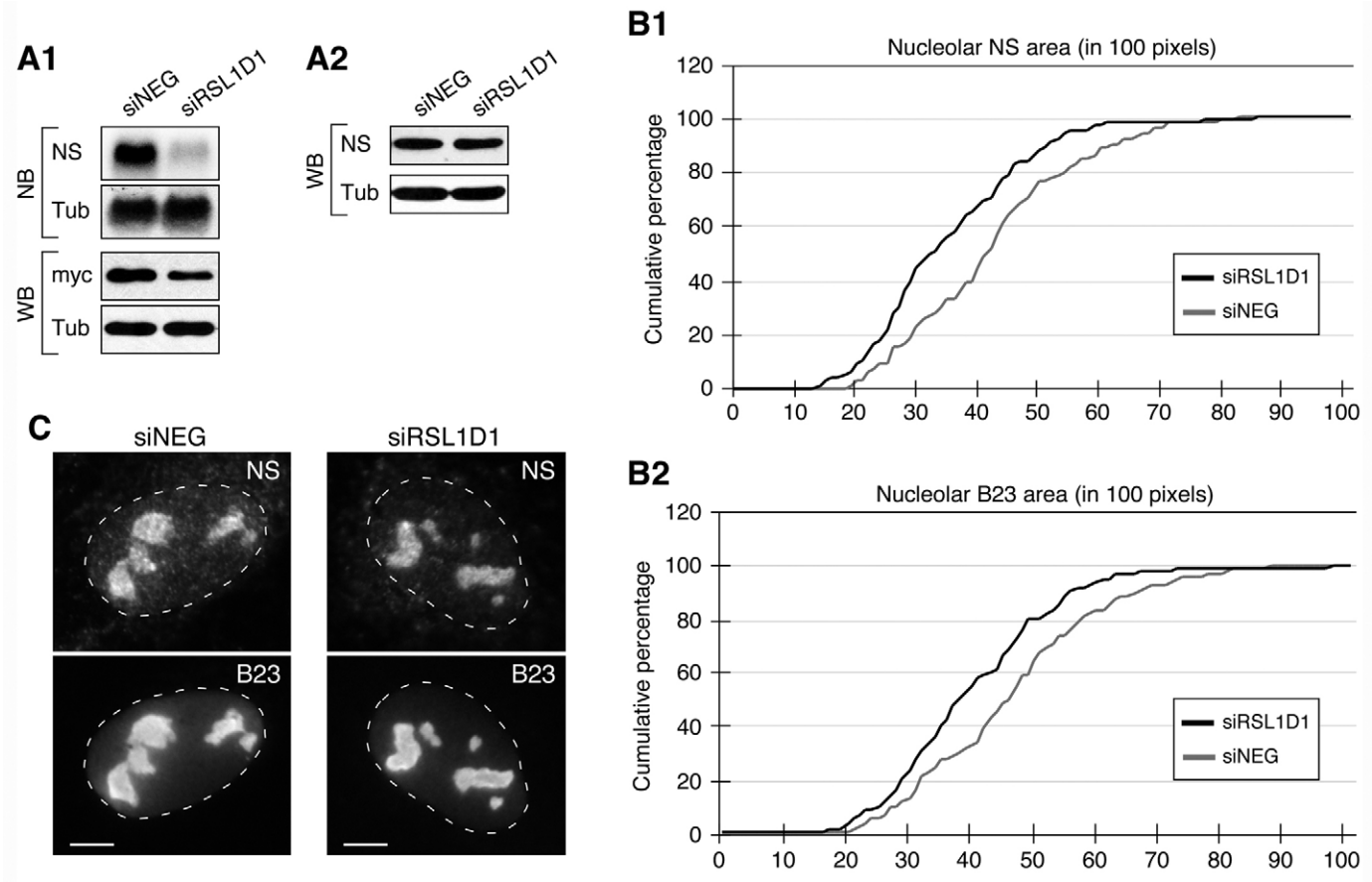

Fig. 9. Loss of RSL1D1 expression decreases the compartmental size and protein amount of nucleostemin and B23 in the nucleolus. (A1) The knockdown efficiency of the RSL1D1-specific siRNA duplex (siRSL1D1) was examined at the RNA and protein levels. Compared with samples treated with the control siRNA duplex (siNEG), siRSL1D1 can reduce the endogenous *RSL1D1* mRNA by 73% (top panel), and the exogenously expressed Myc-tagged RSL1D1 protein by 43% in HEK293 cells (bottom panel). The siRSL1D1 treatment does not affect the total amount of nucleostemin protein (A2). Tub, β-tubulin for northern blots (NB), and α-tubulin for western blots (WB). The effect of a partial loss of RSL1D1 expression on the nucleolar distribution of nucleostemin was measured in U2OS cells double-labeled with anti-nucleostemin (Ab2438) and anti-B23 antibody. Quantitative analyses show that a partial knockdown of RSL1D1 expression decreased the total nucleolar area (No) occupied by nucleostemin (B1) ($P<0.001$, $n=130$). A similar effect was seen in the B23-containing regions (B2). On the *y*-axis the percentage of cells at or below the size indicated on the *x*-axis is shown. On the *x*-axis the nucleoluar area in units of 100 pixels (equals 0.89 μm^2) is shown. (C) Immunofluorescence images representative of the average of each group are shown. Dashed lines delineate the nucleo-cytoplasmic boundaries. Bars, 5 μm.

Table 1. siRNA knockdown of RSL1D1 (siRSL1D1), its effect on nucleolar distributions of nucleostemin and B23, nuclear size and number of nucleoli per cell

	Nucleostemin				B23				Nuclear area (per 100 pixels*)	Nucleoli per cell
	No (per 100 pixels*)	No/Nu (%)	N/P	NoxN/P	No (per 100 pixels*)	No/Nu(%)	N/P	NoxN/P		
siRSL1D1	35.0±1.2	14.1±0.4	3.4±0.1	118.8±5.4	40.2±1.3	16.3±0.4	3.5±0.1	136.5±5.2	247.1±5.6	4.3±0.1
siNEG	42.4±1.3	16.8±0.4	3.2±0.1	131.6±4.5	46.3±1.4	18.4±0.4	3.3±0.1	152.9±5.9	251.4±5.1	4.5±0.1
P-value	<0.001	<0.001	0.09	0.05	<0.001	<0.001	0.14	0.02	0.54	0.14

No, nucleolar area.
No/Nu, nucleolar-to-nuclear area.
N/P, ratio of nucleolar-to-nucleoplasmic fluorescence intensity.
NoxN/P, overall immunofluorescence of the nucleolus relative to its nucleoplasmic fluorescence intensity.
siNEG, control siRNA targeting a scrambled sequence.
*, 100 pixels equal 0.89 μm^2.
P-values were calculated by *t*-test.

from the signal intensities and distribution patterns, neither fibrillarin (Fig. 8C) nor B23 (Fig. 8D) was affected by nlsL1 overexpression. These results show that nlsL1 might function as a dominant-negative regulator for the nucleolar distribution of nucleostemin.

Partial loss of RSL1D1 expression decreases the nucleolar distribution of nucleostemin

Because the RSL1D1-interacting domains of nucleostemin coincide with nucleolar localization regions, but the nucleostemin-interacting domain and the nucleolus-targeting domain of RSL1D1 are distinctively separated, we reason that the nucleolar distribution of nucleostemin might be secondary to that of RSL1D1. To test this idea, we knocked down the expression of RSL1D1 using the small interfering RNA (siRNA) approach and examined the distribution of nucleostemin. Compared with the control siRNA (siNEG) knockdown samples, treatment with RSL1D1-specific siRNA (siRSL1D1) reduced the *RSL1D1* expression by 73% at the RNA level and 43% at the protein level, but did not affect the total protein level of nucleostemin (Fig. 9A). siRSL1D1-treated cells showed a mild but significant decrease in the nucleolar size defined by the nucleostemin signal (Fig. 9B1, 9C, and Table 1). The nucleostemin-positive nucleolar area (No) and the ratio of this area to the total nuclear area (No/Nu) in siRSL1D1-treated cells were 35.0±1.2 (per 100 pixels) and 14.1±0.4%, compared with siNEG-treated cells at 42.4±1.3 (per 100 pixels) and 16.8±0.4% ($P<0.001$, $n=130$). Although siRSL1D1 treatment produced a statistically insignificant ($P=0.09$) increase in the nucleolar fluorescence intensity of nucleostemin relative to its nucleoplasmic fluorescence intensity (N/P), the overall immunofluorescence of nucleostemin in the nucleolus relative to its nucleoplasmic fluorescence intensity (NoxN/P) was still decreased by the RSL1D1 knockdown ($P=0.05$). No difference was seen in the total nuclear area and the number of nucleolus per cells between the siRSL1D1-treated and siNEG-treated samples, indicating that these nucleolar phenotypes were not caused by sampling errors or by changes in the overall cell condition (Table 1). To determine whether siRSL1D1 knockdown interferes with other nucleolar proteins, we immunolabeled B23 in the same sets of cells stained with anti-nucleostemin antibody. Our analyses showed that siRSL1D1 also reduced the nucleolar occupancy of B23, measured by the size of the nucleolus, the ratio of the nucleolar and nuclear size, and the total fluorescence in the nucleolus (Fig. 9B2, 9C, and Table 1). Together, these results show that a partial loss of RSL1D1 expression reduces the amount of nucleostemin and B23 in the nucleolus.

Discussion

This study is designed to understand the mechanism that regulates the distribution of nucleostemin between the nucleolus and the nucleoplasm. Our data reveal a complex model that involves nucleolar and nucleoplasmic components, as well as distinct domains of nucleostemin (Fig. 10). The nucleolar localization of nucleostemin is mediated by its B- and G-domains, and blocked by its I-domain. This I-domain-mediated nucleoplasmic-retaining mechanism does not depend on the B- or the G-domain, but is disabled by the GTP-bound G-domain. Without the I-domain, the G-domain is localized in the nucleolus regardless of its GTP-binding state. Nucleostemin interacts with an L1-domain-containing gene, *RSL1D1*, identified by a yeast two-hybrid screen. Nucleostemin and RSL1D1 colocalize in the same subnucleolar compartment. The interaction between these two proteins requires the B- and G-domains of nucleostemin on one hand and a non-nucleolar, non-L1-domain-containing region of RSL1D1 (aa 317-452) on the other hand. Overexpression of a nucleolar RSL1D1 mutant lacking the nucleostemin-binding ability (nlsL1) disperses the nucleostemin signal from the nucleolus. A partial loss of RSL1D1 expression reduces mostly the compartmental size but also the protein amount of nucleostemin in the nucleolus.

The B-domain and the G-domain of nucleostemin display two distinctively different nucleolar retention properties. It is unclear why two domains with different retention kinetics are needed for the nucleolar localization of nucleostemin. One possibility is that the short retention signal (the B-domain) is used to fine-tune the long retention signal (the G-domain). When both domains are present (NSdA), its FRAP signal becomes less than that of the GI-domain only during the very late phase of the recovery (Fig. 1C3). Another possibility is that the B-domain and the G-domain take part in different biological activities coordinated by nucleostemin. At the molecular level, we were unable to distinguish the B- and the G-domain by their interacting partners. Both domains bind the same nucleolar protein, RSL1D1. Notably, the interaction between the G-domain and RSL1D1 also requires the N-terminal 73 aa of the I-domain, which contains the G2 and G3

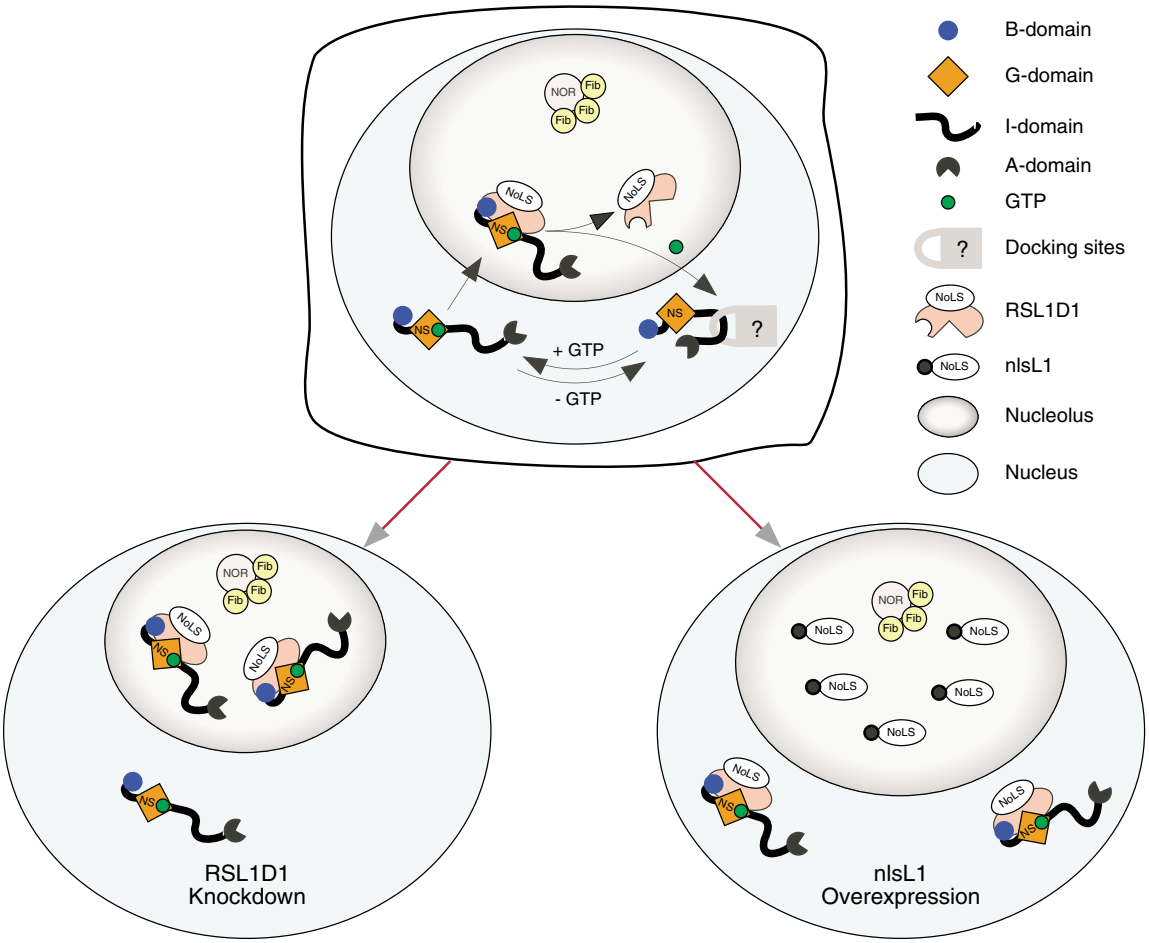

Fig. 10. Diagram of the mechanism controlling nucleostemin distribution between the nucleolar and nucleoplasmic compartments, and the effects of RSL1D1 knockdown and nlsL1 overexpression. Nucleostemin in the GTP-unbound state is blocked from entering the nucleolus by a nucleoplasmic-retaining mechanism that acts on the I-domain. GTP binding releases this lock and allows nucleostemin to move into the nucleolus. Nucleostemin interacts with nucleolar protein RSL1D1 through the nucleolus-targeting B- and G-domains. When not bound by GTP, the GI-domain fails to interact with RSL1D1, suggesting a link between the nucleolar exit of nucleostemin and GTP hydrolysis. RSL1D1 co-resides with nucleostemin in subnucleolar domains surrounding fibrillarin. A partial knockdown of RSL1D1 expression reduces the compartmental size and, to a lesser extent, the protein amount of nucleostemin in the nucleolus, supporting the idea that RSL1D1 provides the nucleolar binding site for nucleostemin. Overexpression of nlsL1 disperses nucleostemin signals from the nucleolus by occupying the nucleolar binding sites for the endogenous RSL1D1 capable of interacting with nucleostemin. NoLS, nucleolar localization sequence(s); NOR, nucleolar organization region; Fib, fibrillarin.

GTP-binding motifs that are less conserved and shorter than the G4 and G1 motifs. To molecularly dissect the different domains of nucleostemin and RSL1D1, some truncated mutants are inevitably left without an NLS. Since nuclear translocation is a prerequisite step for initiating nucleolar localization after the protein is synthesized, we used an SV40 NLS to bring those mutant proteins into the nucleus. Although we have shown that this SV40 NLS alone is not sufficient to confer nucleolar distribution (Fig. 1B, nlsHd3), it may still cooperate with and enhance the activity of the NoLS of nucleostemin to a different degree when compared to the NLS of nucleostemin. This might explain why the G-domain can enter the nucleolus when tagged with an SV40 NLS, but is unable to bind RSL1D1 by itself.

RSL1D1 represents a nucleolar component that regulates the nucleolar localization of nucleostemin. At the molecular level, the nucleolus-targeting and RSL1D1-interacting activities of nucleostemin are encoded by the same domains, whereas the nucleolus-targeting and nucleostemin-binding domains of RSL1D1 are different. At the functional level, the nucleolar retention time of RSL1D1 is longer than that of the full-length nucleostemin and resembles the FRAP recovery kinetics of the GI-domain. Overexpression of an RSL1D1 mutant, nlsL1, can disperse the nucleostemin signal from the nucleolus. Since the nucleolar nlsL1 cannot bind nucleostemin, this mutant may occupy the nucleolar binding sites for endogenous RSL1D1, and functions as a dominant-negative regulator for the nucleolar nucleostemin. A partial loss of RSL1D1 expression reduces the nucleostemin-defined nucleolar size by 18%. Although the nucleostemin signal intensity in the nucleolus appeared elevated, the overall nucleostemin fluorescence signal in the nucleolus of siRSL1D1-treated cells was still reduced by 10% compared with the siNEG-treated cells (P=0.05). The changes in the nucleostemin distribution associated with the

siRSL1D1 treatment are mild, which might be owing to an incomplete knockdown effect. It is difficult to assess the efficiency of siRSL1D1 treatment at the endogenous protein level without an anti-RSL1D1 antibody. Notably, the siRSL1D1 treatment also reduces the nucleolar distribution of B23, suggesting that RSL1D1 directly regulates the nucleolar distribution of B23, or affects B23 indirectly through nucleostemin. This finding also indicates that the nucleolus is composed of different compartments that are interconnected with one another. Together, these results support the in vivo importance of RSL1D1 in regulating the nucleolar localization of nucleostemin.

Given the role of RSL1D1 in the nucleolar distribution of nucleostemin and that RSL1D1 cannot bind the GTP-unbound GI mutant [Fig. 6C; GI(256)], the timing of the dissociation between nucleostemin and RSL1D1, as well as the nucleolar exit of nucleostemin, might be triggered by the GTP hydrolysis of nucleostemin. GTP hydrolysis is a tightly regulated biological event for all GTP-binding proteins. Nucleostemin belongs to a subfamily of GTPases containing a MMR_HSR1 domain in the Pfam database. Unlike the Ras protein, all members in this subfamily have four GTP-binding motifs arranged in a circularly permuted order, where the G4 motif is localized N-terminally to the G1, G2 and G3 motifs (Daigle et al., 2002; Leipe et al., 2002). To date, only one gene in this family in multicellular organisms has been experimentally shown to contain some intrinsic GTPase activities (Reynaud et al., 2005). To address if the nucleolar exit of nucleostemin is triggered by GTP hydrolysis, we generated a Pro258Val mutation in nucleostemin that corresponded to the position of the mutation in the constitutively active GTPase activity in the human RAS mutant [RAS(G12V)]. However, our NS(P258V) mutant failed to yield a constitutively active phenotype regarding its GTP-binding or nucleolar retention property, indicating that some fundamental differences in the GTP-binding structures exist between the MMR_HSR1 family and the small GTPase family.

The modular property of nucleostemin provides a molecular basis for predicting the roles of proteins that interact with different parts of nucleostemin. For example, a protein that binds the B- and/or G-domains might mediate the nucleolar targeting/retention step of nucleostemin or might be transported to the nucleolus by nucleostemin, or might act downstream of the nucleolar functions of nucleostemin. Supporting this idea, we have shown that the B- and G-domain-interacting RSL1D1 is involved in the nucleolar localization of nucleostemin. Human *RSL1D1* was previously identified as one of the genes that are inhibited by cellular senescence (GenBank accession numbers AAN41298 and AY154473), or overexpressed in the non-small-cell lung cancer (GenBank accession number AAT06742) or in human trophoblast cells (CAA07491). Similarly, nucleostemin is highly expressed by several types of human cancer cells (Liu et al., 2004; Tsai and McKay, 2002), and its expression is suppressed in mouse embryonic fibroblast cells undergoing cellular senescence (Zhu et al., 2006). RSL1D1 displays a wider distribution than nucleostemin during embryogenesis and in adult mice. The fact that some tissues express RSL1D1 but not nucleostemin suggests that it may also work as a nucleolar hub for proteins other than nucleostemin. Proteins interacting with the I-domain remain unidentified at this moment. They are expected to serve as the nucleoplasmic docking sites for nucleostemin. The nucleoplasmic-retaining activity of the I-domain does not depend on the B- or G-domains, suggesting that it can be used by other nucleolar proteins. A BLAST search of the GenBank database identifies only two protein sequences that share significant homologies with the I-domain of nucleostemin. They belong to the guanine nucleotide binding protein-like 3 (nucleolar)-like (*Gnl3l*) and Ngp1 (*Gnl2*) genes, which represent the closest family members for nucleostemin in vertebrates. It will be interesting to see whether those nucleoplasmic docking sites, once identified, are free-floating or tethered to the nuclear matrix and whether all nucleostemin family genes share the same docking molecule.

In conclusion, we show that the dynamic distribution of nucleostemin between the nucleolus and the nucleoplasm is controlled by a combination of nucleolar and nucleoplasmic mechanisms. This work raises the idea that partitioning of nucleolar proteins between subnuclear compartments employs complex molecular devices to achieve a specific, rapid and reversible response.

Materials and Methods

Recombinant plasmids and site-directed mutagenesis

Deletions and point mutations were introduced by the stitching PCR method as described previously (Tsai and McKay, 2002; Tsai and McKay, 2005). The final PCR products were subcloned into pCIS expression vectors and confirmed by sequencing. Full-length *RSL1D1* cDNAs were cloned from mouse embryonic stem cells and human MCF7 cells by reverse-transcription PCR.

Cell culture, transfection and immunostaining

Three different cell lines, which all expressed nucleostemin, were used in this study. HEK293 cells were used for biochemical studies because of their high transfection efficiency and protein production. U2OS cells were used for subcellular distribution analysis because of their large and flat-shaped nuclei. CHO cells were used for the FRAP experiments because of their simple nucleolar morphology. Cells were maintained in Dulbecco's modified Eagle's medium (DMEM) supplemented with 5% fetal bovine serum (FBS; Hyclone), penicillin (50 IU/ml), streptomycin (50ug/ml), and glutamine (1%). Plasmid transfections were performed using a standard calcium phosphate method for HEK293 cells or Lipofectamine-Plus reagents (Invitrogen) for U2OS cells, and analyzed 2 days after transfection. Immunofluorescence studies were performed as described previously (Tsai and McKay, 2005). Cells were fixed with fresh 4% paraformaldehyde on ice for 15 minutes. Primary antibodies included: affinity-purified polyclonal Ab2438 (1:500; chicken IgY) for endogenous nucleostemin, monoclonal anti-HA antibody (1:2000; HA.11, Covance), monoclonal anti-myc antibody (1:1000; 9E10, Covance), monoclonal anti-fibrillarin antibody (1:1000; 38F3, EnCor), and monoclonal anti-B23 antibody (1:1000, Zymed). Secondary antibodies were conjugated with Red-X or FITC.

Yeast two-hybrid screen

A sequence containing the GTP-binding and the intermediate domains (GI) of rat nucleostemin (aa 106-459) was subcloned in the pAS2-1 vector as a bait to screen a 7-day-old mouse embryo cDNA library in pACT2 (Clontech). The bait and library plasmids were co-transformed into *Saccharomyces cerevisiae* strain Y190 and selected for both histidine$^+$ and β-galactosidase$^+$ phenotypes. cDNA plasmids were electroporated into *Escherichia coli* HB101 and amplified for sequencing.

Coimmunoprecipitation

Cells were harvested in NTEN buffer (20 mM Tris pH 8.0, 150 mM NaCl, 1 mM EDTA, 0.5% NP40, 0.1 mM DTT, supplemented with 1 mM PMSF, 1 μg/ml leupeptin, 0.5 μg/ml aprotinin, 0.7 μg/ml pepstatin A, and 1 μM E64). Lysates were incubated with monoclonal anti-HA (HA.11, Covance), monoclonal anti-Myc (9E10, Covance) or polyclonal anti-nucleostemin (Ab1164) antibodies for 1 hour at 4°C, followed by incubation with protein-G sepharose beads (Pharmacia) for another 4 hours at 4°C. Immunoprecipitates were washed five times with RIPA buffer (1× PBS, 0.1% SDS, 0.5% sodium deoxycholate, 1% NP40, 1 mM PMSF, 1 μg/ml leupeptin, 0.5 μg/ml aprotinin, 0.7 μg/ml pepstatin A, and 1 μM E64), fractionated by 10% SDS-PAGE, and transferred to Hybond-P membranes (Amersham). Specific signals were detected by western blot analyses using

polyclonal anti-HA or anti-Myc primary antibodies and horseradish peroxidase-conjugated secondary antibodies.

GST pull-down assay

Full-length and partial cDNAs of RSL1D1 and nucleostemin were subcloned into the pGEX4T-2 vector. GST fusion proteins were expressed in BL21/DE3 as described previously (Tsai and McKay, 2002). Epitope-tagged proteins were expressed in HEK293 cells and extracted in PBS–Triton-X-100 (1%) buffer, supplemented with protease inhibitors. Sepharose-bound GST fusion proteins (2 μg) were incubated with cell lysates for 2 hours at 4°C, washed five times with extraction buffer, including twice with high-salt solutions (500 mM NaCl), fractionated on 10% SDS-PAGE and detected by western blottings.

Northern blot analyses

Ten micrograms of total RNAs were isolated from CD-1 mice using Trizol solutions (Invitrogen), fractionated on a 1% formamide denaturing agarose gel, and transferred onto Hybond XL membrane (Amersham). Filters were then hybridized with α-^{32}P-labeled probes at 65°C overnight and washed with high-stringency buffer. Plaque date was counted as embryonic day 0.5 (E0.5).

siRNA knockdown

siRNA duplexes were designed to target the sense sequence 5′-AGTGGTTCTTGCAGTGCTA-3′ in the human RSL1D1 gene and a scrambled sequence 5′-TGACGATCAGAATGCGACT-3′ (Dharmacon). Cells were transfected with siRNA duplexes (100 nM) for 15 hours using the Oligofectamine reagent (Invitrogen), and fixed with 4% paraformaldehyde 3 days after transfection. The distributions of endogenous nucleostemin and B23 were detected by anti-nucleostemin (Ab2438) and anti-B23 immunofluorescence and counterstained with DAPI.

FRAP analysis

CHO cells grown in Nalgene Lab Tek II chamber slides were transfected with 0.6 μg plasmid DNA using Lipofectamine-Plus reagents 1 day before the measurement. Bleaching experiments were performed on a Zeiss LSM510 confocal microscope with a 63× plan-apochromat oil objective. The photobleaching protocol was modified based on previous reports (Dundr et al., 2000; Phair and Misteli, 2000). The GFP signal was excited with the 488 nm argon laser (20 mW nominal output), and emission was monitored above 505 nm. Cells were maintained at 35°C with a heat blower throughout the entire procedure. A spot of 1 μm in diameter was bleached within the nucleolus using a short laser pulse administered at 100% power for three iterations. All experiments were ensured to achieve 70-80% bleaching of the original intensity. For image acquisition, the laser power was attenuated to 0.6% of the bleach intensity, and cells were scanned with 5× zoom at 0.29-second intervals for 31.6 seconds after photobleaching. For quantification, fluorescence intensities of the region of interest, the entire nucleus, and the outside of the nucleus were measured. Signal recovery in the bleached area (FRAP) was normalized to the total intensity in the nucleus after background subtraction and averaged over 20 cells from three independent experiments. Cells with a signal loss of more than 10% during the imaging phase were not used.

Image acquisition and analyses

Confocal images were captured on a Zeiss LSM510 confocal microscope using a 63× plan-apochromat oil objective. In Fig. 2, images were scanned with a 512×512 frame size, 2× zoom, and <1.4 μm optical thickness. For high-resolution studies (Figs 4, 8, and supplementary material Fig. S2), images were scanned with a 512×512 frame size and 4× zoom. Optical slices of 0.7 μm were sampled by setting the pinhole size at less than 1 Airy unit. Detector gain and amplifier offset were adjusted to ensure all signals were appropriately displayed within the linear range. Immunofluorescent images were captured on a Zeiss Axiovert 200 microscope using a 63× plan-apochromat oil objective and a CoolSNAP*EZ* Monochrome camera (Photometrics, 6.45×6.45-μm pixels). Exposure time was set so that the brightest intensity reached 80% of the saturation intensity. For the siRNA experiments, captured images were analyzed using the ImageJ 1.36b software (http://rsb.info.nih.gov/ij/). The nucleolar size, the ratio of nucleolar-to-nuclear area, and the ratio of nucleolar-to-nucleoplasmic (N/P) fluorescence intensity were measured from 130 cells randomly sampled from seven independent experiments in a double-blind study. All nucleolar regions within a single cell were delineated. The average intensities of the whole nucleolar and nucleoplasmic areas were calculated to generate the N/P intensity ratio. Areas were measured in pixels (100 pixels equal 0.89 μm^2).

We thank Seokwoon Kim and Qubo Zhu for their technical support of this work. This project is supported by TIRR/Mission Connect startup fund and R01 CA113750-01 to R.Y.T.

References

Andersen, J. S., Lam, Y. W., Leung, A. K., Ong, S. E., Lyon, C. E., Lamond, A. I. and Mann, M. (2005). Nucleolar proteome dynamics. *Nature* **433**, 77-83.

Baddoo, M., Hill, K., Wilkinson, R., Gaupp, D., Hughes, C., Kopen, G. C. and Phinney, D. G. (2003). Characterization of mesenchymal stem cells isolated from murine bone marrow by negative selection. *J. Cell. Biochem.* **89**, 1235-1249.

Bernardi, R., Scaglioni, P. P., Bergmann, S., Horn, H. F., Vousden, K. H. and Pandolfi, P. P. (2004). PML regulates p53 stability by sequestering Mdm2 to the nucleolus. *Nat. Cell Biol.* **6**, 665-672.

Carmo-Fonseca, M., Mendes-Soares, L. and Campos, I. (2000). To be or not to be in the nucleolus. *Nat. Cell Biol.* **2**, E107-E112.

Chen, D. and Huang, S. (2001). Nucleolar components involved in ribosome biogenesis cycle between the nucleolus and nucleoplasm in interphase cells. *J. Cell Biol.* **153**, 169-176.

Daigle, D. M., Rossi, L., Berghuis, A. M., Aravind, L., Koonin, E. V. and Brown, E. D. (2002). YjeQ, an essential, conserved, uncharacterized protein from Escherichia coli, is an unusual GTPase with circularly permuted G-motifs and marked burst kinetics. *Biochemistry* **41**, 11109-11117.

Dundr, M., Misteli, T. and Olson, M. O. (2000). The dynamics of postmitotic reassembly of the nucleolus. *J. Cell Biol.* **150**, 433-446.

Fox, A. H., Lam, Y. W., Leung, A. K., Lyon, C. E., Andersen, J., Mann, M. and Lamond, A. I. (2002). Paraspeckles: a novel nuclear domain. *Curr. Biol.* **12**, 13-25.

Leipe, D. D., Wolf, Y. I., Koonin, E. V. and Aravind, L. (2002). Classification and evolution of P-loop GTPases and related ATPases. *J. Mol. Biol.* **317**, 41-72.

Liu, S. J., Cai, Z. W., Liu, Y. J., Dong, M. Y., Sun, L. Q., Hu, G. F., Wei, Y. Y. and Lao, W. D. (2004). Role of nucleostemin in growth regulation of gastric cancer, liver cancer and other malignancies. *World J. Gastroenterol.* **10**, 1246-1249.

Martel, C., Macchi, P., Furic, L., Kiebler, M. A. and Desgroseillers, L. (2006). Staufen1 is imported into the nucleolus via a bipartite nuclear localization signal and several modulatory determinants. *Biochem. J.* **393**, 245-254.

Mekhail, K., Gunaratnam, L., Bonicalzi, M. E. and Lee, S. (2004). HIF activation by pH-dependent nucleolar sequestration of VHL. *Nat. Cell Biol.* **6**, 642-647.

Mekhail, K., Khacho, M., Carrigan, A., Hache, R. R., Gunaratnam, L. and Lee, S. (2005). Regulation of ubiquitin ligase dynamics by the nucleolus. *J. Cell Biol.* **170**, 733-744.

Misteli, T. (2005). Going in GTP cycles in the nucleolus. *J. Cell Biol.* **168**, 177-178.

Olson, M. O. and Dundr, M. (2005). The moving parts of the nucleolus. *Histochem. Cell Biol.* **123**, 203-216.

Pederson, T. (1998). The plurifunctional nucleolus. *Nucleic Acids Res.* **26**, 3871-3876.

Phair, R. D. and Misteli, T. (2000). High mobility of proteins in the mammalian cell nucleus. *Nature* **404**, 604-609.

Politz, J. C., Lewandowski, L. B. and Pederson, T. (2002). Signal recognition particle RNA localization within the nucleolus differs from the classical sites of ribosome synthesis. *J. Cell Biol.* **159**, 411-418.

Politz, J. C., Polena, I., Trask, I., Bazett-Jones, D. P. and Pederson, T. (2005). A nonribosomal landscape in the nucleolus revealed by the stem cell protein nucleostemin. *Mol. Biol. Cell* **16**, 3401-3410.

Reed, M. L., Dove, B. K., Jackson, R. M., Collins, R., Brooks, G. and Hiscox, J. A. (2006). Delineation and modelling of a nucleolar retention signal in the coronavirus nucleocapsid protein. *Traffic* **7**, 833-848.

Reynaud, E. G., Andrade, M. A., Bonneau, F., Ly, T. B., Knop, M., Scheffzek, K. and Pepperkok, R. (2005). Human Lsg1 defines a family of essential GTPases that correlates with the evolution of compartmentalization. *BMC Biol.* **3**, 21.

Rubbi, C. P. and Milner, J. (2000). Non-activated p53 co-localizes with sites of transcription within both the nucleoplasm and the nucleolus. *Oncogene* **19**, 85-96.

Rubbi, C. P. and Milner, J. (2003). Disruption of the nucleolus mediates stabilization of p53 in response to DNA damage and other stresses. *EMBO J.* **22**, 6068-6077.

Sheng, Z., Lewis, J. A. and Chirico, W. J. (2004). Nuclear and nucleolar localization of 18-kDa fibroblast growth factor-2 is controlled by C-terminal signals. *J. Biol. Chem* **279**, 40153-40160.

Sleeman, J. E., Trinkle-Mulcahy, L., Prescott, A. R., Ogg, S. C. and Lamond, A. I. (2003). Cajal body proteins SMN and Coilin show differential dynamic behaviour in vivo. *J. Cell Sci.* **116**, 2039-2050.

Tsai, R. Y. (2004). A molecular view of stem cell and cancer cell self-renewal. *Int. J. Biochem. Cell Biol.* **36**, 684-694.

Tsai, R. Y. and McKay, R. D. (2002). A nucleolar mechanism controlling cell proliferation in stem cells and cancer cells. *Genes Dev.* **16**, 2991-3003.

Tsai, R. Y. and McKay, R. D. (2005). A multistep, GTP-driven mechanism controlling the dynamic cycling of nucleostemin. *J. Cell Biol.* **168**, 179-184.

Weber, J. D., Taylor, L. J., Roussel, M. F., Sherr, C. J. and Bar-Sagi, D. (1999). Nucleolar Arf sequesters Mdm2 and activates p53. *Nat. Cell Biol.* **1**, 20-26.

Wong, J. M., Kusdra, L. and Collins, K. (2002). Subnuclear shuttling of human telomerase induced by transformation and DNA damage. *Nat. Cell Biol.* **4**, 731-736.

You, J., Dove, B. K., Enjuanes, L., DeDiego, M. L., Alvarez, E., Howell, G., Heinen, P., Zambon, M. and Hiscox, J. A. (2005). Subcellular localization of the severe acute respiratory syndrome coronavirus nucleocapsid protein. *J. Gen. Virol.* **86**, 3303-3310.

Zhu, Q., Yasumoto, H. and Tsai, R. Y. (2006). Nucleostemin delays cellular senescence and negatively regulates TRF1 protein stability. *Mol. Cell. Biol.* (in press).